Hydrogen-Peroxide-Enhanced Nonthermal Plasma Effluent for Biomedical Applications

Marek Gołkowski, *Member, IEEE*, Czesław Gołkowski, Jori Leszczynski, S. Reed Plimpton, Piotr Masłowski, Aleksandra Foltynowicz, Jun Ye, and Bruce McCollister

***Abstract*—A novel nonthermal plasma dielectric-barrier discharge (DBD) system for decontamination, sterilization, and medical applications has been developed. The discharge is physically removed from the disinfection zone, and plasma-induced free radicals are delivered through an air stream. The physical distance between the discharge and the treatment surface can be up to 3 m, making the technology robust and flexible for applications in the medical clinic. The bactericidal properties of the free-radical effluent are enhanced by hydrogen peroxide additives. We report a 6-log reduction in *Staphylococcus aureus* and *Pseudomonas aeruginosa* bacteria strains in under 1 min of exposure *in vitro* and inactivation of *Bacillus atrophaes* spores and *Escherichia coli* biofilms. The concentration of hydrogen peroxide additives is seen to be a key variable in inactivation efficacy, suggesting that active species in our experiment may be different than in other DBD configurations. Precise chemical concentration measurements using direct frequency comb spectroscopy show presence of ozone (O_3), hydrogen peroxide (H_2O_2), nitrous oxide (N_2O), and nitrogen dioxide (NO_2). *In vivo* multiple exposures of mouse skin to the plasma effluent do not yield any adverse effects.**

***Index Terms*—Bacteria, biomedical, decontamination, frequency comb spectroscopy, plasma medicine, reactive oxygen species (ROS).**

I. Introduction

THE USE of nonthermal gas discharge plasmas in disinfection, sterilization, and various biomedical applications has received considerable attention in the last decade. Review articles written by Laroussi [1] and Moreau *et al.* [2] describe the major technical approaches that have been pursued to effectively inactivate a wide range of microorganisms. Specifically, there is an established distinction between so-called "direct" and "indirect" (or remote) methods of using plasma discharges in biological applications [3]. In direct methods, the target to be decontaminated or treated is physically present in the discharge region. Such direct treatment is most commonly accomplished using a dielectric-barrier discharge (DBD), where the target is a floating electrode. In indirect methods, the treatment target is physically removed from the discharge, and chemical species created in the discharge are transported to the sample by forced flow or diffusion. The advantage of direct methods is that all active species generated in a plasma discharge, including those with very short lifetimes such as free electrons, ions, hydroxyl radicals, and also UV photons, can participate in the decontamination and maximize its effectiveness. However, direct methods are inherently sensitive to the geometry of the treatment sample and, therefore, are not as robust and flexible as indirect methods in the context of applications to tissue or instrument surfaces in the medical clinic.

The need for robust and flexible engineering solutions is all the more relevant as, recently, there have been significant promising advancements in animal studies [4], [5] and also clinical studies of nonthermal plasma treatments on human patients [6], [7]. Kuo *et al.* [4] show evidence of air plasma treatments reducing wound bleeding, whereas Ermolaeva *et al.* [5] employ an argon plasma device to achieve a statistically significant increase in the rate of wound closure. Perhaps most significantly, two studies by Isbary *et al.* [6], [7] demonstrate that plasma treatments are effective in reducing bacterial load on chronic wounds and in treating Hailey–Hailey disease in human patients. The aforementioned clinical studies involve direct treatment hardware with capital costs in the range of tens to hundreds of thousands of dollars.

A recent comprehensive study by Joshi *et al.* [8] confirms previous results that hydrogen peroxide (H_2O_2) is readily generated in air plasmas and is an active species contributing to bacteria inactivation through lipid peroxidization. The bactericidal properties of H_2O_2 in plasma treatments have led to efforts to increase its concentration by direct addition. Yamamoto *et al.* [9] investigated injection of H_2O_2 droplets in a corona discharge and concluded that the H_2O_2 additive was one of the dominant reactive species in their sterilization experiment. It is also worth noting that sterilization technologies based on vaporized H_2O_2 have been developed by companies such as STERIS Corporation [10].

The device described herein is an indirect exposure approach with hydrogen peroxide additives that generates a plasma-induced free-radical air stream. We report sterilization results

Manuscript received November 30, 2011; revised March 25, 2012 and May 8, 2012; accepted May 8, 2012. Date of publication June 12, 2012; date of current version August 7, 2012. The works of M. Gołkowski, A. Foltynowicz, and P. Masłowski were supported by the University of Colorado Denver Faculty Development, the Swedish Research Council postdoctoral fellowship, and the Polish Ministry of Science and Higher Education, respectively.

M. Gołkowski is with the Department of Electrical Engineering and the Department of Bioengineering, University of Colorado Denver, Denver, CO 80217 USA.

C. Gołkowski is with Super Pulse, Ithaca, NY.

J. Leszczynski is with the Department of Pathology and the Office of Laboratory Animal Resources, University of Colorado Denver, Denver, CO 80217 USA.

S. Reed Plimpton is with the Department of Bioengineering, University of Colorado Denver, Aurora, CO 80045-2560 USA.

P. Masłowski, A. Foltynowicz, and J. Ye are with the JILA, NIST and the University of Colorado Boulder, Boulder, CO 80309-0440 USA.

B. McCollister is with the Infectious Diseases Division and the Department of Microbiology, University of Colorado Denver, Aurora, CO 80045 USA.

Color versions of one or more of the figures in this paper are available online at http://ieeexplore.ieee.org.

Digital Object Identifier 10.1109/TPS.2012.2200910

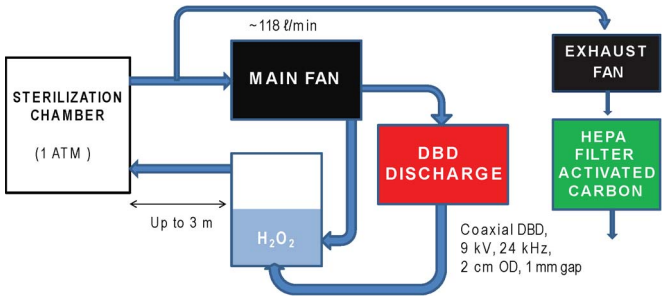

Fig. 1. Block diagram of device components and effluent flow.

comparable to direct methods achieved with low-cost hardware and flexibility in application. In an *in vivo* experiment, we demonstrate that exposure to our effluent on the time scales necessary for high-level disinfection does not create adverse effects to murine skin. We use direct frequency comb absorption spectroscopy to obtain precise real-time measurements of the concentrations of ozone (O_3), hydrogen peroxide (H_2O_2), nitrous oxide (N_2O), and nitrogen dioxide (NO_2) in our effluent.

II. Device Description

The plasma device described herein is an upgraded version of an earlier setup described by Watts *et al.* [11] with the key exception that microwave discharge has been replaced with DBD, and a closed-loop flow has been implemented. Fig. 1 shows the flow diagram and main components of the system. The closed-loop flow system allows for maximum buildup of concentration of free radicals and reactive oxygen species (ROS). Two identical 100-W fans provide circulation (main fan) and exhaust (exhaust fan). The role of the exhaust fan is to keep the closed-loop system in a state of under pressure preventing any escape of free radicals or pathogens except through the exhaust exit, which contains an activated carbon ROS deactivation bed and a HEPA filter. It is, thus, possible to operate the device without the need for a chemical hood or a biosafety cabinet despite the relatively copious concentrations of ROS discussed below. Flow from the main fan is split one third to the DBD and two thirds bypassing the DBD and directly connecting to the hydrogen peroxide bubbler. The DBD component consists of two independent units, each with two concentric cylindrical electrodes. The length of the cylindrical electrodes is 15 cm. The outer diameter of the outer electrode is 2 cm with a 1-mm electrode gap. The two DBD units are in parallel in the context of the airflow. Each DBD unit is driven by a 9-kV-amplitude 24-kHz-voltage waveform. After the DBD, the flow streams connect and proceed to the hydrogen peroxide bubbler. The bubbler contains 50% H_2O_2 solution by mass. The wicking material prevents any droplets from being carried by the effluent stream into the sterilization chamber. The sterilization chamber can be up to 3 m from the bubbler exit. The flow rate through the system is 118 L/min, and the temperature is $\sim$25 °C. The inner diameter of the tubing connecting the main components is 2.06 cm made from Teflon and vinyl. Although operation of the device with DBD enabled but without hydrogen peroxide solution or with hydrogen peroxide solution but with DBD disabled yields a bactericidal effluent, superior bacteria inactivation rates are achieved with both components active.

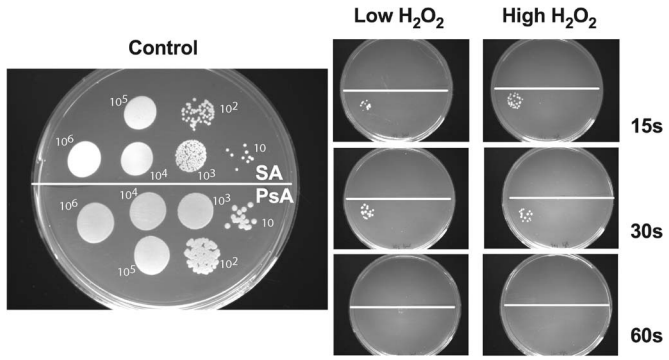

Fig. 2. Agar plates inoculated with indicated concentrations of *Staphylococcus aureus* (SA) and *Pseudomonas aeruginosa* (PsA) after exposure to the plasma effluent for indicated duration and 24-h incubation. The left plate marked control was not exposed. The concentration and bacteria strain indicated on the control plate apply to the corresponding location on all plates. "High H_2O_2" and "Low H_2O_2" designations refer to the heating of the hydrogen peroxide solution, as described in the text.

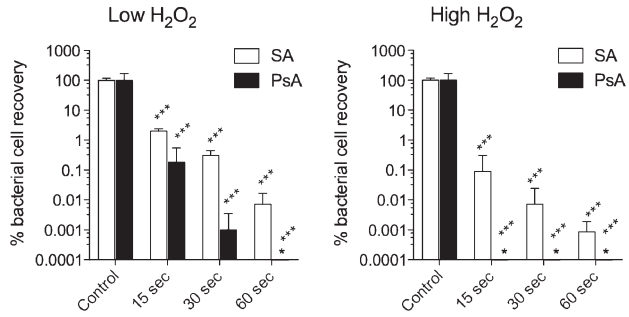

Fig. 3. Survival of *Staphylococcus aureus* (SA) and *Pseudomonas aeruginosa* (PsA) on plastic badges after exposure to the plasma effluent for various times. Data are presented as % bacterial cell recovery +/− standard deviation. *** ($p < 0.001$ compared with SA or PsA controls by two-way ANOVA of transformed data with Bonferroni's post-test). "High H_2O_2" and "Low H_2O_2" designations refer to the heating of the hydrogen peroxide solution, as described in the text.

III. Biological Tests

A. In Vitro Tests

The antimicrobial properties of the effluent were tested on *Staphylococcus aureus* and *Pseudomonas aeruginosa* bacteria strains on agar plates. The agar plates were inoculated with six distinct concentrations [10, 10^2, 10^3, 10^4, 10^5, and 10^6 colony forming units (CFUs)] of both types of bacteria, as shown in the left control panel in Fig. 2. The plates were exposed to the plasma effluent for durations of 15, 30, and 60 s. Exposure involved placement in a 2-L-volume plastic sterilization chamber connected to the closed-loop flow as in the Fig. 1 diagram. After exposure, all plates including the unexposed control were incubated overnight at 37 °C. Fig. 2 shows that 15 s of exposure was sufficient to inactivate all concentrations of *Staphylococcus aureus*. For the *Pseudomonas aeruginosa* strain, the results are similar except that the 10^6 original concentration spot is seen to require 60 s of exposure to be completely inactivated. For the exposures denoted by "High H_2O_2" in Fig. 2, the hydrogen peroxide bubbler was heated to a temperature of 40 °C, whereas for the "Low H_2O_2" exposures, the hydrogen peroxide was left at room temperature. The same designations apply to results shown in Fig. 3 and discussed

below. Although the results with the heated hydrogen peroxide solution are shown for completeness, and it is noteworthy that they yield higher inactivation rates than without heating, condensation of hydrogen peroxide solution was observed under this setting. Since such condensation is undesirable for most medical applications, particularly those involving live tissue, we believe that the results for the room-temperature setting ("Low H_2O_2") are more clinically relevant.

In a second more quantitative experiment, *Staphylococcus aureus* and *Pseudomonas aeruginosa* were inoculated on plastic identification badges of the type often worn by medical personnel. We note that a similar study of disinfection of personal pagers was recently performed by Burts *et al.* [12]. The badges were chosen as an inoculation medium since such objects are known to be a major vector for pathogen transmission and are currently not subject to any satisfactory disinfection/sterilization procedures. Each badge was inoculated with four spots of 10^6 CFU of *Staphylococcus aureus* and *Pseudomonas aeruginosa*. The badges were exposed for durations of 15, 30, and 60 s. Dampened cotton swabs were used to remove the bacteria and placed in a 2-mL lysogeny broth (LB) medium. The cultures were serially diluted in phosphate-buffered saline, spotted on LB agar plates, and the viable bacteria enumerated after overnight incubation at 37 °C. Fig. 3 shows data presented as percent of bacterial cell recovery in reference to the unexposed control group. Focusing on the "Low H_2O_2" results in the left panel in Fig. 3, it is shown that a 15-s exposure results in a 2-log reduction in culturable bacteria (1% recovery), and a 60-s exposure results in a 4-log reduction (0.01% recovery) for *Staphylococcus aureus* and a 6-log reduction (0.0001% recovery) for *Pseudomonas aeruginosa*. It is useful to compare these results with those obtained by Burts *et al.* [12] who also used an indirect plasma exposure method to sterilize pagers but report much lower inactivation rates. Specifically, in [6, Fig. 1], it is shown that for the same initial bacterial concentrations (10^6 CFU), an 80%–95% survival results after a 60-s exposure with their device, and a 20%–35% survival results after a 10-min exposure. Our device is thus able to achieve inactivation rates orders of magnitude higher than other indirect devices and on par with direct methods such as those used by Fridman *et al.* [3]. Specifically, exposure to our effluent for times of less than a minute yields high-level disinfection as defined by the FDA to be a 6-log reduction in viable pathogens. Such a reduction is believed to eliminate enough pathogens to prevent infection [13].

In a third *in vitro* test, the plasma-induced free-radical effluent produced by our device was applied to bacteria in a spore form as pathogens in this dormant survival state are hard to eradicate. The hardiness of the spores also provides an opportunity to quantitatively assess the effects of the different components of our device. Fig. 4 shows the results of *Bacillus atrophaes* spores (10^6 CFU) after exposure to our effluent for 5 min under five different operational modes. The control group was not exposed. For the "plasma only" mode, we operated the device without any solution in the evaporator. For the "plasma + water" mode, water was placed in the bubbler in place of the hydrogen peroxide solution. For the "H_2O_2 only" mode, hydrogen peroxide solution was placed in the evaporator, but the DBD was not activated. The "plasma + H_2O_2" mode is

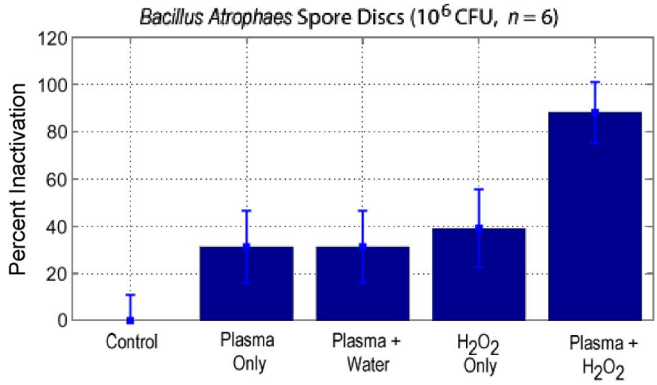

Fig. 4. Results from the experiment of exposure of *Bacillus atrophaes* spores for 5 min showing the effect of deactivation of various components of the device. A 90% inactivation rate is only achieved when both plasma discharge and hydrogen peroxide solution are used together.

our normal operational mode and included both DBD and hydrogen peroxide solution as in the previously described bacteria tests. The sample size for each mode was six spore discs, and the evaporator was always at room temperature. The best inactivation rate (close to 90%) occurs for the "plasma + H_2O_2" mode, whereas the other noncontrol modes yield inactivation rates in the range of 30%–40%. The fact that the most effective combination for pathogen deactivation involves both DBD and hydrogen peroxide solution suggests that there is significant coupling between the chemical species generated in the DBD and H_2O_2.

In a final *in vitro* test, we investigated the efficacy of our device in biofilm inactivation. Biofilms are difficult to eradicate because of an extracellular matrix that protects the individual bacterial cells. Since biofilms are responsible for a significant portion of nosocomial infections in the clinical setting, there is a need for new technologies capable of effective biofilm inactivation. Biofilm samples were prepared from *Escherichia coli* in multiwell culture plates containing six wells with a volume of 16.8 mL and a surface area of 9.5 cm^2 per well. For these tests, we did not use the closed-loop flow of the device and set up the culture plate so that a well in the corner was directly exposed to the effluent flow. The two wells on the plate opposite from the exposed well were covered with a glass slide. The exposure time was 5 min, and the experiment was repeated three times. The geometry of the plate and exposure scheme is shown in the top panel in Fig. 5. The lower panel in Fig. 5 shows the average CFUs recovered from each well, as well as from control wells that were not exposed. The results from the directly exposed well show that 5 min of exposure leads to a 6-log reduction of culturable cells in the biofilm. The adjacent wells experience a 2–3-log reduction, whereas the covered cells are essentially not affected. The effluent produced by our device is effective against biofilms, but it is necessary that the target be fully immersed in the effluent. Dilution of the effluent as occurred in the case of wells 2–4 in Fig. 5 quickly reduces its effectiveness. These results confirm the importance of the closed-loop flow design used in the other biological tests since this ensures delivery of the effluent to all parts of the sterilization chamber and prevents its dilution.

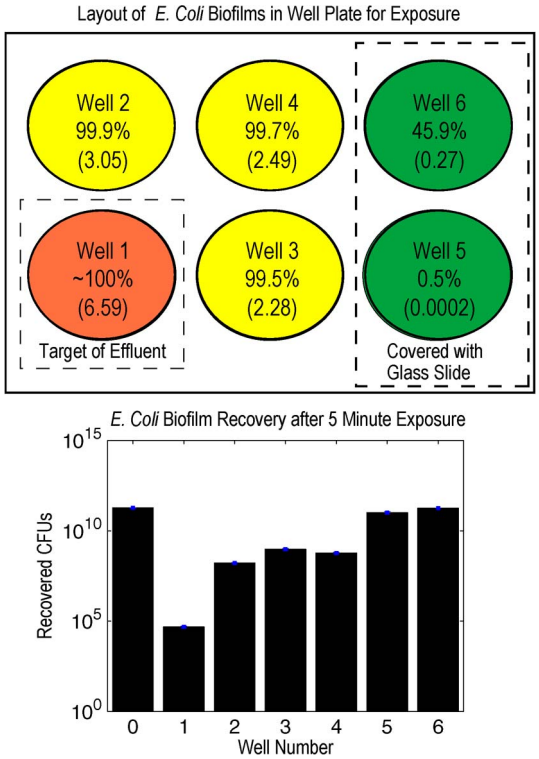

Fig. 5. Results from the experiment with *Escherichia coli* biofilms prepared in multiwell culture plates. The top panel shows the layout of the wells in a six-well plate. The output of the device was directed at well 1; wells 5 and 6 were covered with a glass slide. The exposure time was 5 min, and the experiment was repeated three times. The numbers in each well indicate the percentage of CFUs inactivated and the corresponding log reduction averaged over three repetitions of the experiment. The bottom panel shows a graph of average recovery of CFUs from each well. The control (well 0) was not exposed to the device effluent.

B. In Vivo Tests

Having shown that the plasma-induced effluent produced in our device is capable of achieving sterilization on time scales suitable for clinical application, the effect of the effluent on live tissue was explored in a test involving live mice. Such tests are important for all applications of plasma technology to live tissue, including wound treatments or simple alternatives to hand washing. Fig. 6 shows the special sterilization chamber that was designed allowing exposure of the body of the mice but preventing exposure of the head so that the mice would not inhale the plasma effluent. Four groups of eight CD-1 (both male and female) mice each had their backs shaved the night before the start of the experiment. Shaving allowed for maximum exposure of the skin to the effluent. The first group was a control group, which was not exposed to the effluent. The subsequent groups were exposed to the effluent for 30-s durations once per day, three times per day, and five times per day, respectively. The exposures were separated by at least 1 h, and the mice were briefly sedated with isoflurane anesthesia during the exposure. The experiment lasted for three days after which the skin of the mice was grossly examined by one of us (J. Leszczynski, University of Colorado Veterinarian). Panel (c) in Fig. 6 shows the skin of a mouse from the control group, and panel (d) shows the skin of a mouse from the group exposed to five 30-s treatments per day for five days. From gross examination,

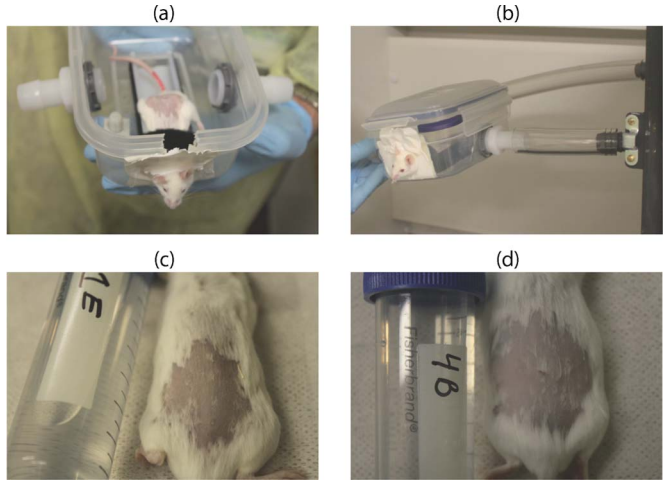

Fig. 6. Photographs from the *in vivo* experiment. (a) Mouse in a special sterilization vessel. (b) Sterilization vessel with the mouse connected to the device. (c) Skin of the control-group mouse. (d) Mouse exposed to five daily 30-s treatments hourly spaced for three days.

none of the mice exposed to the plasma showed any signs of inflammation or redness as compared with the control group. The only notable damage to the skin was from small cuts from the shaving process, which were also observed on the control group. All studies were performed under a protocol approved by the University of Colorado Institutional Animal Care and Use Committee.

IV. Analysis of Chemical Composition

The chemical composition of the effluent from our device was investigated using direct frequency comb absorption spectroscopy at JILA, NIST and the University of Colorado Boulder. This technique is currently at the leading edge of tools for trace gas detection requiring broadband coverage and rapid acquisition times [14], [15]. It provides high sensitivity and selectivity to molecular absorption combined with broad wavelength coverage necessary for multispecies detection [16]. The source of light in our direct frequency comb spectroscopy experimental setup is a midinfrared optical parametric oscillator (OPO) [17] pumped by a high-power femtosecond Yb:fiber laser at 1064 nm [18]. The optical spectrum of the OPO spans 150 nm around a center wavelength continuously tunable between 2.8 and 4.6 μm. The plasma effluent is flown through a multipass Herriott cell, in which the interaction length between the sample and the optical beam is 18 m. The multipass optical cell was modified so that it could be connected into the closed-loop flow of the device in place of the sterilization chamber shown in Fig. 1. The volume of the multipass cell is $\sim$0.3 L so that the conditions in the glass optical cell and the plastic sterilization chambers we used for the tests described above are expected to be identical. The light exiting the multipass cell is analyzed with a fast-scanning Fourier transform interferometer [19], [20].

What makes the direct frequency comb spectroscopy particularly useful for the investigation herein is the capability to simultaneously measure concentrations of multiple species to a high degree of precision with short acquisition time (less

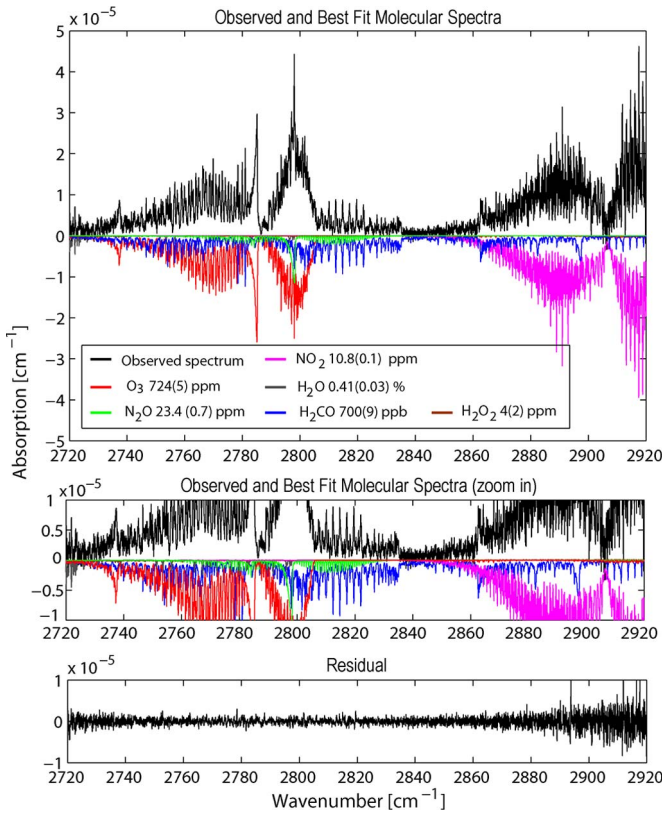

Fig. 7. Top panel shows the absorption spectrum of the plasma effluent (black curve) at 620-torr pressure measured around 3.6 μm (2800 cm^{-1}) at time $t =$ 140 s from the left panel in Fig. 8. The individual molecular spectra, whose sum is fitted to the measured data, are plotted inverted for clarity, and an expanded y-axis is displayed in the middle panel. The residual of the fit (observed minus best fit spectrum) is shown in the bottom panel. The concentration of each gas calculated from the fit is displayed in the legend in the top panel, where the uncertainty (one standard deviation) is shown in parenthesis.

than 1 s) even in the presence of significant concentrations of water ($\sim$1%). The operation in the mid-IR wavelength range gives access to strong fundamental transitions of numerous molecular species [19] and provides high absorption sensitivity. In order to detect the molecules present in the plasma effluent $(O_3, H_2O_2, NO_2, N_2O)$, the center wavelength of the OPO was tuned to 3.6 or 3.7 μm. An example of an absorption spectrum of the plasma effluent at pressure 620 torr measured around 3.6 μm (2800 cm^{-1}) is shown in black in the top panel in Fig. 7. The concentration of each gas is determined from a fit of a sum of known molecular spectra from the HITRAN molecular database, with gas concentrations as fitting parameters. The individual molecular spectra shown in Fig. 7 are inverted for clarity, and an expanded absorption vertical axis is shown in the middle panel. The residual of the fit is displayed in the bottom panel, indicating excellent recovery of quantitative information of relevant chemical species.

Fig. 8 shows the results from two measurement series, both with (right) and without (left) hydrogen peroxide solution in the evaporator. The average steady-state concentrations of ozone (O_3), hydrogen peroxide (H_2O_2), nitrous oxide (N_2O), and nitrogen dioxide (NO_2) for full operation (DBD and main pump activated) are summarized above the plots. The uncertainty in concentration (represented as one standard deviation) corresponds to the detection limit for the particular molecule.

The addition of the hydrogen peroxide solution to the DBD discharge raises the H_2O_2 concentration from below the detection limit to $\sim$400 ppm. The concentration of NO_2 remains roughly constant irrespective of whether the device is operated with hydrogen peroxide. The concentrations of N_2O and O_3 are found to decrease by a factor of 2 with the addition of hydrogen peroxide. In both cases, the device requires about 10 s to reach saturation levels of the major chemical species. This quick attainment of free-radical and ROS saturation, which required considerable engineering of the fans and the evaporator to maintain a high flow rate, is likely one of the key reasons that the device is able to achieve much faster pathogen inactivation than other indirect methods.

V. Discussion

Currently, the two main areas of effort in nonthermal plasma biomedical applications are understanding the exact mechanisms of pathogen inactivation and optimizing hardware solutions for specific medical applications. The primary mechanism of pathogen inactivation by nonthermal plasma-induced chemistry can be caused by multiple factors including erosion of the cell wall, interference with the cell inner membrane, or DNA damage [21], [22]. None of these mechanisms occur in isolation, and it has been shown that ROS can interact with the cell inner membrane via lipid peroxidation, which can cause the cells to leak and also create reactive byproducts that can subsequently lead to DNA damage [8]. Although polyunsaturated lipids, which are the main substrate for lipid peroxidation, are found in low levels in bacteria membranes, a growing number of experiments have reported lipid peroxidation as a mechanism of bacteria cellular damage under exposure to ROS [23]–[25]. Most relevant to the mechanisms induced by our device, a comprehensive study by Joshi *et al.* [8] investigated the effect of ROS produced by nonthermal plasma and found evidence that ROS scavengers such as vitamin E were able to prevent the extent of lipid peroxidation.

Although atmospheric pressure plasma discharges can produce a wide range of ROS, the DBD in our device is seen to produce mainly ozone, and comparable concentrations of H_2O_2 are achieved by direct addition through our bubbler. The reduction potential of both O_3 and H_2O_2 is sufficient for direct peroxidation (oxidative degradation) of lipids in a cell membrane, but the most oxidizing radical is known to be the hydroxyl radical (OH^*) [26]. The interaction of O_3 and H_2O_2 can favorably produce hydroxyl radicals (OH^*) in what is called a peroxone process [27], i.e.,

$$H_2O_2 + 2O_3 \rightarrow 2OH^* + 3O_2.$$

Unfortunately, the peroxone process is difficult to quantify in our device as it requires a surface or a liquid phase since O_3 and H_2O_2 are not expected to interact in the gas phase directly. In this context, we note that a subsequent measurement with the spectrometer tuned to the fundamental band of the hydroxyl radical near 2.9 μm did not show any OH^* presence within the detection limits of the system. An experiment using direct frequency comb spectroscopy to investigate surface chemistry

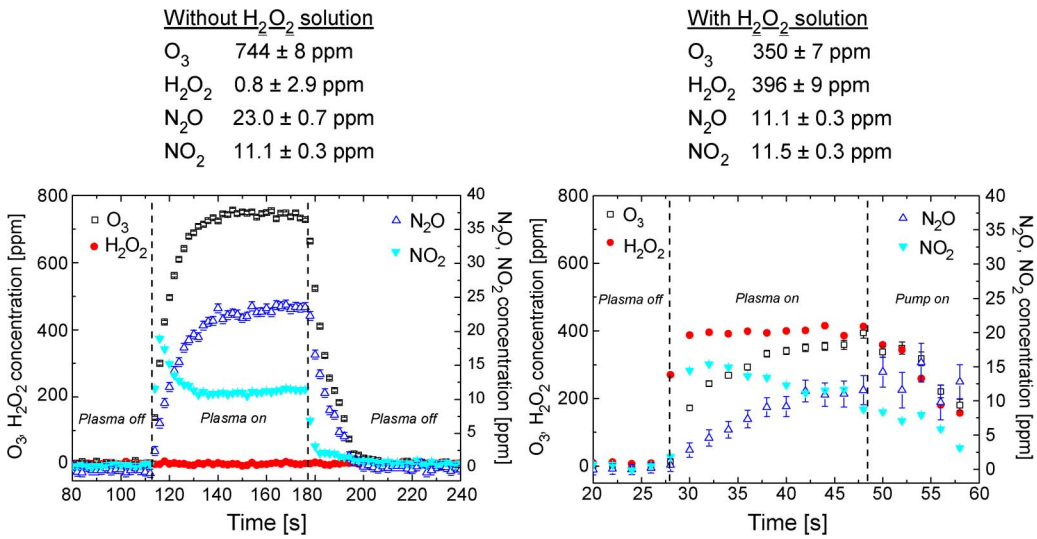

Fig. 8. Time dependence of chemical species concentrations measured with direct frequency comb spectroscopy as the device (DBD and fans) are turned on and off.

is being considered for the near future. Hydroxyl radicals are also readily produced by reduction cleavage of H_2O_2 by a reduced metal as in the well-known Fenton reaction [26], i.e.,

$$Fe^{2+} + H_2O_2 \rightarrow Fe^{3+} + OH^* + OH^-.$$

Our device's ability to inactivate pathogens and spores on short time scales is likely due to the production of hydroxyl radicals at the biological target made possible by the presence of H_2O_2. Hydroxyl radicals produced from the interaction between ozone and H_2O_2 are a possible reason for the results in Fig. 4, where the DBD discharge and hydrogen peroxide in unison produce the most effective inactivation results. We note that ozone, by itself, cannot be the main inactivation agent since, as shown in Fig. 8, its concentration is lowered by a factor of 2 with the addition of hydrogen peroxide solution. We also note that hydroxyl radicals do not have sufficient lifetimes at atmospheric pressure to be able to reach the sterilization chamber of our device if they are directly produced in the discharge. An electron spin resonance experiment might be able to provide direct evidence of the generation of hydroxyl radicals from other ROS at the target surface upon exposure to our effluent.

Nonthermal plasmas have been seen to be slightly less effective in deactivating gram-positive bacteria than gram-negative bacteria because of a difference in the cell envelope structure [22]. The cell envelope of gram-negative microorganisms is a multilayer system composed of an inner cytoplasmic membrane made of phospholipids and proteins, a peptidoglycan layer, and an outer membrane of poly polymers such as polysaccharides. Gram-positive cells have a less complex envelope with a thicker peptidoglycan layer and the general absence of the outer membrane. As discussed above, recent works have emphasized bactericidal effects of ROS such as ozone and hydrogen peroxide to occur via disruption of envelope integrity through peroxidation of phospholipids and lipoproteins found in the inner membrane of both gram-negative and gram-positive cells. In our results, gram-negative *Pseudomonas aeruginosa* proved more resistant on agar plates (see Fig. 2) but less resistant on plastic badges (see Fig. 3) when compared with gram-positive *Staphylococcus aureus*.

We note that any interaction between the ROS produced in our device and the inner cell membrane will require passage of these species through the outer membrane and the peptidoglycan structure. It has been documented that inactivation rates of nonthermal plasma technologies depend not only on the type of bacteria but also on the type of the medium supporting the microorganisms [21]. The plastic badges represent a harsh environment with no extra nutrients in contrast to the nutrient-rich conditions on the agar plates. It is possible that *Pseudomonas aeruginosa* and *Staphylococcus aureus* differently respond to these environments in terms of their ability to directly resist ROS or perform cell repair or ROS mitigation processes. We also note that the bacteria on the agar plates were plated about an hour before exposure. Such a period of time in a nutrient-rich environment might have allowed the bacteria to direct their genome to a more biofilm type of growth, with potential differences between the two strains again playing a role. Although our device is effective against biofilms (see Fig. 5), the deactivation process requires longer time scales. The production of hydroxyl radicals OH^* on the surface of either cell type by either the peroxone or Fenton processes discussed above is not able to be quantified at this time, although it is also of fundamental importance.

An important ROS species that we were not able to measure with our spectrometer is nitric oxide (NO), which can play a role in wound healing by inducing fibroblast proliferation and regulating immune deficiencies [28]. The NO absorption band at 2.8 μm overlaps with a strong absorption band of water, and another absorption band at 5 μm is outside the operating frequency range of the OPO. A new frequency comb source that will cover this spectral region is under development. In terms of chemistry dynamics, we note that the concentrations of the nitrogen oxides and other active species such as ozone are all coupled. For example, nitrous oxide (N_2O) gives rise to NO (nitric oxide) on reaction with oxygen atoms, and NO, in turn, reacts with ozone to produce nitrogen dioxide (NO_2). The

multiple and simultaneous reactions make numerical modeling of the chemical dynamics difficult, hence the need for direct measurement of simultaneous concentrations, which is a capability that the frequency comb spectroscopy uniquely provides.

The operational parameters of our device utilized in these experiments (flow rate and plasma discharge) were empirically arrived upon to produce the quickest possible pathogen inactivation rates, which we have presented above. The effects of the course variation of parameters, namely, the presence of the hydrogen peroxide solution and the activation/deactivation of the plasma discharge, are shown in Fig. 4 (spore inactivation) and in Fig. 8 (chemical concentrations). A high flow rate is key in quickly achieving the high concentrations of ROS in the sterilization chamber and is the maximum the current hardware can supply. For a fixed geometry and flow rate, atmospheric pressure nonthermal plasmas have a small window of stable operation, therefore making significant variations of the discharge voltage unlikely to improve performance. A quantitative model of dominant chemical processes including the generation of OH^* radical production will allow for future optimization of the technology.

VI. Conclusion

The hydrogen-peroxide-enhanced nonthermal plasma effluent produced in our device has shown for the first time that pathogen inactivation on time scales previously associated with direct plasma treatments is possible with an indirect plasma treatment. The free-radical effluent has been shown to be also effective against bacteria in the spore state and biofilms and does not produce adverse effects on mammalian tissue on time scales necessary for clinical application. The hardware for our plasma device is significantly cheaper than that of plasma treatments being used in clinical trials. The lower hardware cost and flexibility of application afforded by an indirect treatment make the technology ripe for application in the medical clinic.

Acknowledgment

The authors would like to thank Super Pulse for the experiment hardware and the NIST and AFOSR for the measurements at JILA.

References

[1] M. Laroussi, "Nonthermal decontamination of biological media by atmospheric-pressure plasmas: Review, analysis, and prospects," *IEEE Trans. Plasma Sci.*, vol. 30, no. 4, pp. 1409–1415, Aug. 2002.

[2] M. Moreau, N. Orange, and M. G. J. Feuilloley, "Non-thermal plasma technologies: New tools for bio-decontamination," *Biotechnol. Adv.*, vol. 26, no. 6, pp. 610–617, Nov./Dec. 2008.

[3] G. Fridman, A. D. Brooks, M. Balasubramanian, A. Fridman, A. Gutsol, V. N. Vasilets, H. Ayan, and G. Friedman, "Comparison of direct and indirect effects of non-thermal atmospheric-pressure plasma on bacteria," *Plasma Process. Polym.*, vol. 4, no. 4, pp. 370–375, 2007.

[4] S. P. Kuo, C.-Y. Chen, C.-S. Lin, and S.-H. Chiang, "Wound bleeding control by low temperature air plasma," *IEEE Trans. Plasma Sci.*, vol. 30, no. 4, pp. 1409–1415, Aug. 2002.

[5] S. A. Ermolaeva, A. F. Varfolomeev, M. Y. Chernukha, D. S. Yurov, M. M. Vasiliev, A. A. Kaminskaya, M. M. Moisenovich, J. M. Romanova, A. N. Murashev, I. I. Selezneva, T. Shimizu, E. V. Sysolyatina, I. A. Shaginyan, O. F. Petrov, E. I. Mayevsky, V. E. Fortov, G. E. Morfill, B. S. Naroditsky, and A. L. Gintsburg, "Bactericidal effects of non-thermal argon plasma *in vitro*, in biofilms and in the animal model of infected wounds," *J. Med. Microbiol.*, vol. 60, pp. 75–83, Jan. 2011.

[6] G. Isbary, G. Morfill, H. U. Schmidt, M. Georgi, K. Ramrath, J. Heinlin, S. Karrer, M. Landthaler, T. Shimizu, B. Steffes, W. Bunk, R. Monetti, J. L. Zimermann, R. Pompl, and W. Stolz, "A first prospective randomized controlled trial to decrease bacterial load using cold atmospheric argon plasma on chronic wounds in patients," *Brit. J. Dermatol.*, vol. 163, no. 1, pp. 78–82, Jul. 2010.

[7] G. Isbary, G. Morfill, J. L. Zimermann, T. Shimizu, and W. Stolz, "A successful treatment of lesions in Hailey–Hailey disease," *Arch. Dermatol.*, vol. 147, no. 4, pp. 388–390, 2011.

[8] S. G. Joshi, M. Cooper, A. Yost, M. Paff, K. Ercan, G. Fridman, G. Friedman, A. Fridman, and A. D. Brooks, "Nonthermal dielectric-barrier discharge plasma-induced inactivation involves oxidative DNA damage and membrane lipid peroxidation in *Escherichia coli*," *Antimicrobial Agents Chemotherapy*, vol. 55, no. 3, pp. 1053–1062, Mar. 2011.

[9] M. Yamamoto, M. Nishioka, and M. Sadakata, "Sterilization using a corona discharge with H_2O_2 droplets and examination of effective species," *J. Electrostat.*, vol. 55, no. 2, pp. 173–187, Jun. 2002.

[10] A. Kahnert, P. Seiler, M. Stein, B. Aze, G. McDonnell, and S. H. E. Kaufmann, "Decontamination with vaporized hydrogen peroxide is effective against *Mycobacterium tuberculosis*," *Lett. App. Microbiol.*, vol. 40, no. 6, pp. 448–452, Feb. 2005.

[11] A. E. Watts, S. L. Fubini, M. Vernier-Singer, C. Gołkowski, S. Shin, and R. J. Todhunter, "In vitro analysis of nonthermal plasma as a disinfecting agent," *Amer. J. Vet. Res.*, vol. 67, no. 12, pp. 2030–2035, Dec. 2006.

[12] M. L. Burts, I. Alexeff, E. T. Meek, and J. A. McCullers, "Use of atmospheric non-thermal plasma as a disinfectant for objects contaminated with methicillin-resistant *Staphylococcus aureus*," *Amer. J. Infect. Control*, vol. 37, no. 9, pp. 729–733, Nov. 2009.

[13] W. A. Rutala and D. J. Weber, Healthcare Infection Control Practices Advisory Committee (HICPAC), *Guideline for Disinfection and Sterilization in Healthcare Facilities*, Atlanta, GA, Centers Disease Control Prevention, 2008.

[14] M. J. Thorpe, K. D. Moll, R. J. Jones, B. Safdi, and J. Ye, "Broadband cavity ringdown spectroscopy for sensitive and rapid molecular detection," *Science*, vol. 311, no. 5767, pp. 1595–1599, Mar. 2006.

[15] F. Adler, M. J. Thorpe, K. C. Cossel, and J. Ye, "Cavity-enhanced direct frequency comb spectroscopy: Technology and applications," *Annu. Rev. Anal. Chem.*, vol. 3, pp. 175–205, 2010.

[16] M. J. Thorpe, D. Balslev-Clausen, M. Kirchner, and J. Ye, "Human breath analysis via cavity-enhanced optical frequency comb spectroscopy," *Opt. Exp.*, vol. 16, pp. 2387–2397, 2008.

[17] F. Adler, K. C. Cossel, M. J. Thorpe, I. Hartl, M. E. Fermann, and J. Ye, "Phase-stabilized, 1.5 W frequency comb at 2.8–4.8 μm," *Opt. Lett.*, vol. 34, no. 9, pp. 1330–1332, May 2009.

[18] I. Hartl, T. R. Schibli, A. Marcinkevicius, M. E. Fermann, D. C. Yost, D. D. Hudson, and J. Ye, "Cavity-enhanced similariton Yb-fiber laser frequency comb: 3×10^{14} W/cm^2 peak intensity at 136 MHz," *Opt. Lett.*, vol. 32, no. 19, pp. 2870–2872, Oct. 2007.

[19] F. Adler, P. Masłowski, A. Foltynowicz, K. C. Cossel, T. C. Briles, I. Hartl, and J. Ye, "Mid-infrared Fourier transform spectroscopy with a broadband frequency comb," *Opt. Exp.*, vol. 18, no. 21, pp. 21 861–21 872, Oct. 2010.

[20] A. Foltynowicz, P. Masłowski, T. Ban, F. Adler, K. C. Cossel, T. C. Briles, and J. Ye, "Optical frequency comb spectroscopy," *Faraday Discuss.*, vol. 150, pp. 23–31, 2011.

[21] M. Laroussi, "Low-temperature plasmas for medicine?" *IEEE Trans. Plasma Sci.*, vol. 37, no. 6, pp. 714–725, Jun. 2009.

[22] E. Stoffels, Y. Sakiyama, and D. Graves, "Cold atmospheric plasma: charged species and their interactions with cells and tissues," *IEEE Trans. Plasma Sci.*, vol. 36, no. 4, pp. 1441–1457, Aug. 2008.

[23] J. M. Pérez, F. A. Arenas, G. A. Pradenas, J. M. Sandoval, and C. C. Vásquez, "*Escherichia coli* YqhD exhibits aldehyde reductase activity and protects from the harmful effect of lipid peroxidation-derived aldehydes," *J. Biol. Chem.*, vol. 283, no. 12, pp. 7346–7353, Mar. 2008.

[24] S. J. Yoon, J. E. Park, J.-H. Yang, and J.-W. Park, "*OxyR* regulon controls lipid peroxidation-mediated oxidative stress in *Escherichia coli*," *J. Biochem. Mol. Bio.*, vol. 35, no. 3, pp. 297–301, May 2002.

[25] H. Semchyshyn, T. Bagnyukova, K. Storey, and V. Lushchak, "Hydrogen peroxide increases the activities of *soxRS* regulon enzymes and the levels of oxidized proteins and lipids in *Escherichia coli*," *Cell Biol. Int.*, vol. 29, no. 11, pp. 898–902, Nov. 2005.

[26] G. R. Buettner, "The pecking order of free radicals and antioxidants:lipid peroxidation, α-tocopherol and ascorbate," *Arch. Biochem. Biophys.*, vol. 300, no. 2, pp. 535–543, Feb. 1993.

[27] G. Merényi, J. Lind, S. Naumov, and C. von Sonntag, "Reaction of ozone with hydrogen peroxide (peroxone process): A revision of current mechanistic concepts based on thermokinetic and quantum–chemical considerations," *Environ. Sci. Technol.*, vol. 44, no. 9, pp. 3505–3507, May 2010.
[28] G. Fridman, G. Friedman, A. Gutsol, A. B. Shekhter, V. N. Vasilets, and A. Fridman, "Applied plasma medicine," *Plasma Process. Polym.*, vol. 5, no. 6, pp. 503–533, Aug. 2008.

Marek Gołkowski (M'10) received the B.S. degree in electrical engineering from Cornell University, Ithaca, NY, in 2002 and the M.S. and Ph.D. degrees in electrical engineering from Stanford University, Stanford, CA, in 2004 and 2009, respectively.

From 2009 to 2010, he served as a Postdoctoral Research Fellow with the Space, Telecommunications, and Radioscience Laboratory, Department of Electrical Engineering, Stanford University. He is currently an Assistant Professor with the Department of Electrical Engineering and the Department of Bioengineering, University of Colorado Denver, Denver. He actively conducts research on electromagnetic waves in plasmas, ionospheric physics, near-earth space physics, characterization of antennas in reverberation chambers, hybrid imaging technologies, and biomedical applications of gas discharge plasmas. He has coauthored a fundamental textbook on plasma physics and over 20 journal papers.

Dr. Gołkowski was a recipient of the International Association of Geomagnetism and Aeronomy Young Scientist Award for Excellence in 2008, the IEEE Electromagnetic Compatibility Society Best Symposium Paper Award in 2011, and the American Geophysical Union Outstanding Student Paper Award in Fall 2005. He is an Associate Editor of the journal *Earth*, *Moon*, *Planets*. He is a member of the American Geophysical Union and the International Union of Radio Science (URSI)—Commission H (Waves in Plasmas).

Czesław Gołkowski received the M.S. degree in physics from Silesian University, Katowice, Poland, and the Ph.D. degree in electrical engineering from Cornell University, Ithaca, NY, in 1991.

He served as a Research Associate with the Laboratory of Plasma Studies, Cornell University. He is currently the Founder and President of Super Pulse, an R&D company in Ithaca, NY, that specializes in applications of discharge plasmas for biological and environmental applications. His principal research interests include pulsed power technology, high-power microwave generation, microwave plasma generation, and electrical discharge in gases and its applications. He has published over 25 journal papers and holds two patents.

Jori Leszczynski received the D.V.M. degree from Ohio State University, Columbus, OH, in 1999.

She is currently the Director of the Office of Laboratory Animal Resources, University of Colorado Denver, Denver, and is the University Veterinarian.

S. Reed Plimpton received the B.S. and M.S. degrees in physics from the University of Pennsylvania, Philadelphia, PA, in 2011. He is currently working toward the Ph.D. degree in the bioengineering program at the University of Colorado Denver—Anschutz Medical Campus.

Piotr Masłowski, photograph and biography not available at the time of publication.

Aleksandra Foltynowicz received the M.S. degree in experimental physics from Adam Mickiewicz University, Poznań, Poland, in 2005 and the Ph.D. degree in physics from Umeå University, Umeå, Sweden, in 2009.

From 2010 to 2011, she was a Postdoctoral Research Associate with JILA, University of Colorado, Boulder. She is currently an Assistant Professor with the Department of Physics, Umeå University. Her main field of research is the development and applications of sensitive high-resolution continuous-wave and broadband laser-based absorption spectroscopy techniques. She received the European Physical Society University Student Fellowship in 2003 and the Swedish Research Council Postdoctoral Fellowship in 2009. She has coauthored 18 scientific papers.

Jun Ye received the B.S. degree from Jiao Tong University, Shanghai, China, in 1989; the M.S. degree from the University of New Mexico, Albuquerque, NM, in 1991; and the Ph.D. degree from the University of Colorado, Boulder, in 1997.

Since 2001, he has been a Fellow of JILA, NIST and the University of Colorado. He is a Fellow of NIST, a Fellow of the American Physical Society, a Fellow of the Optical Society of America, and a member of the National Academy of Sciences. His research focuses on the frontier of light–matter interactions and includes precision measurement, quantum physics and cold matters, optical frequency metrology, and ultrafast science and quantum control.

Dr. Ye has coauthored over 250 technical papers and delivered over 330 invited talks. His awards and honors include Frew Fellowship (Australian Academy of Science), I. I. Rabi Prize (APS), European Frequency and Time Forum Award, Carl Zeiss Research Award, William F. Meggers Award and Adolph Lomb Medal (OSA), Arthur S. Flemming Award, Presidential Early Career Award for Scientists and Engineers, U.S. Commerce Department Gold Medals, Friedrich Wilhem Bessel Award (A. von Humboldt Foundation), and Samuel Wesley Stratton Award (NIST). The research group web page is http://jila.colorado.edu/YeLabs/.

Bruce McCollister received the M.D. degree from the University of Minnesota, Minneapolis, MN, in 1995; completed his residency in internal medicine at the University of Colorado School of Medicine in 1998; and the fellowship in infectious diseases at the University of Colorado School of Medicine.

His research in the Department of Microbiology and the Department of Medicine, University of Colorado School of Medicine, is focused on salmonella and bacterial pathogenesis.